Non-destructive characterization of cementitious materials submitted to thermal treatments

Sylvie Masse, Geneviève Vetter, Philippe Boch, C Haehnel

Non-destructive characterization of cementitious materials submitted to thermal treatments

Sylvie Masse[a*], Geneviève Vetter[a], Philippe Boch[a], and C. Haehnel[b]

[a]Ecole Supérieure de Physique et de Chimie Industrielles, F-75231 Paris Cedex 05, France

[b]Association Technique de l'Industrie des Liants Hydrauliques, F-92974 Paris-La Défense, France

Abstract

Cementitious materials (Portland cement pastes, siliceous- or calcareous-sand mortars, and "microconcrete" with silica fume and siliceous sand) were subjected to cumulative thermal treatments, up to 1000°C. Thermal damage was monitored by measuring Young's modulus, using an ultrasonic technique at a frequency of 10 MHz. Complementary characterization methods were mercury porosimetry, X-ray diffraction, scanning electron microscopy, and thermal analysis. The ultrasonic technique is confirmed to be sensitive and reproducible. All the materials exhibit similar trend for relative change in Young's modulus (E/E_0) versus temperature.

Keywords Thermal Treatment (A), Elastic Moduli (C), Degradation (C), Portland Cement (D), Concrete (E)

1. Introduction

Not considering the case of refractory castables, cementitious materials are not expected to endure severe thermal conditions. Accidental fires, however, submit concrete structures to

* Corresponding author. Tel.: 33 (1) 40 79 47 41; fax: 33 (1) 40 79 47 50.

E-mail address: sylvie.masse@espci.fr

high temperatures. Recent examples in Europe were accidental fires in Channel Tunnel (in 1996), Mont-Blanc tunnel and Tauern tunnel (both in 1999), and Kaprun tunnel (in 2000). Temperatures were up to 1000°C. The assessment of damage caused by high-temperature conditions is, therefore, an important question [1,2,3] to address to improve the safety of cementitious structures.

The present study makes a contribution to the problem by studying the effect of cumulative thermal treatments (up to 1000°C) on model materials (cement pastes, mortars, and "microconcretes"). The main technique of characterization was measurement of dynamic Young's modulus (E) by an ultrasonic technique. The technique is non destructive, sensitive, and it gives information on a parameter, E, which is interesting from both an industrial point of view and a scientific point of view. From an industrial point of view, E characterizes the rigidity of a material. From a scientific point of view, E is related to the intensity of interatomic bonds.

Young's modulus experiments were complemented by mercury intrusion porosimetry (MIP), scanning electron microscopy (SEM), X-ray diffraction (XRD), and thermal analyses (DTA/TG).

2. Experimental

2.1. Starting materials

The cement was a Portland cement (CPA CEM I 52.5 CP2 ENV 197-1 NF-P 15-301, NF-P 15-318). Tables 1 and 2 give the chemical analysis and Bogue's composition. Blaine surface area is 3820 $cm^2.g^{-1}$.

Two kinds of sand were used for the preparation of mortars and microconcretes: a siliceous sand with purity of 98.6 % SiO_2 (α-quartz) and grain size of 100-630 µm, and a calcareous one, mainly composed of $CaCO_3$ with a small content of quartz, with grain size of 80-800 µm.

Silica fume with mean grain size of 0.35 µm was used as a filler.

The preparation of mortars and microconcretes was facilitated by adding a polycarboxylate superplasticizer.

2.2. Cement pastes, mortars, and microconcretes

For cement pastes, the water-to-cement (w/c) ratios were 0.25, 0.35, and 0.50. For siliceous mortars, they were 0.35 and 0.50. For calcareous mortars, w/c was 0.50. It must be noted that the preparation of mortars with low-porosity (pore relative volume < 3%) siliceous sand was easier than that of mortars with high porosity (< 12%) calcareous sand. For microconcretes, we only used siliceous sand, with water-to-binder (w/b) ratios of 0.25 and 0.35. The binder was cement for mortars and a mixture of cement with 15% of silica fume for microconcretes.

The mortar and microconcrete materials - approximately 600 g of each composition - were mixed using a stainless-steel container and rotor. First, dry powders were mixed together for ~ ten minutes. The binder-to-sand ratio was of 1-to-3. Then, water (purified using *Elga*® system) and half of total content of superplasticizer were added. After a few minutes, the rest of superplasticizer was added and the mixing was continued for ~ 10 min. The total content of plasticizer was 2% by weight of cement. For cement pastes, we did not add superplasticizer.

Eight sorts of mixes were elaborated: three pastes, three mortars, and two microconcretes. Table 3 gives the nomenclature we used.

2.3. Specimen molding

For each mix, several samples were elaborated in order to check the reproducibility of experiments. For ultrasonic measurement, 3 cylindrical specimens of each composition were molded in Rhodorsil™ silicone (15 mm in diameter and 15-19 mm in height), with vibration at 40 Hz for 10 min. to facilitate degassing. For porosimetry measurements and SEM, several specimens (at least two for each technique) were made by cutting pellets (of approximately

1 cm^3) from bars that had been cast and vibrated in Rhodorsil™ silicone molds (10x10x80 mm). Cutting was made using a circular diamond saw sprayed with ethanol to avoid any change in the hydration degree. DTA/TG and XRD measurements were carried out using finely ground materials.

2.4. Cure and thermal treatment

After 24 hours in molds at room temperature in closed glass-vessel saturated with water, the specimens were demolded and cured for either 7 days or 28 days. Then, the specimens were submitted to cumulative thermal treatments at fixed soaking temperatures.

An electric oven was used for treatments at 80°C, 120°C, 150°C, and 200°C whereas an electric muffle furnace was used for treatments at higher temperatures of 250°C, 300°C, 400°C, 500°C, 600°C, 700°C, 800°C, and 1000°C. In the oven, the thermal program was heating at 0.2°C.min^{-1} up to the chosen temperature, soaking for 10 h, and natural cooling. In the furnace, the rate of heating was 3.0°C.min^{-1} up to the temperature that had been reached in the previous treatment, then heating at 0.2°C.min^{-1} up to new soaking temperature. Soaking time was still of 10 h, followed by natural cooling.

We have to point out that our purpose was to study the changes experienced by a *material*, not to evaluate the damage suffered by a *structure*. To collect materials data, it is better to be close to an equilibrium state, which explains the choice of small-size specimens and of low heating rates. The studies conducted on thermal shock behavior of brittle materials (glass, ceramics and cementitious materials) have shown that the best approach [4] is that of decoupling the variables. Transient effects, in particular thermal gradients and, therefore, differential strains, can be studied using numerical methods (for instance 3D finite elements), which are fed with the relevant materials data. They have to be complemented by experimental studies on bulky specimens, in particular to take into account spalling and effects of pore pressure [5] .

2.5. Ultrasonic characterization

Elasticity in isotropic solid is characterized by two moduli, Young's modulus (E) and shear modulus (G). Poisson's ratio (ν) is also used, with:

$$G = \frac{E}{2(1+\nu)} \qquad \text{Eq. (1).}$$

For acoustic waves traveling through an infinite isotropic medium, the longitudinal-wave velocity (v_l, in $m.s^{-1}$) is related to E, ν, and ρ (apparent bulk density, in $kg.m^{-3}$), by:

$$E = \rho\, v_l^2\, \frac{(1+\nu)(1-2\nu)}{(1-\nu)} \qquad \text{Eq. (2)}$$

To estimate the two parameters E and G, one has to measure both v_l (velocity of longitudinal waves) and v_s (velocity of shear waves). However, Poisson's ratio is much less sensitive than E to structural changes, as long as the material remains in the "solid state", since shear waves do not propagate within a non-viscous liquid. This means physical and chemical changes in materials can be followed by measuring Young's modulus only, with the assumption that Poisson's ratio keeps rather a constant value. Poisson's ratio was found [6] to be 0.27 ± 0.03 for Portland compositions with total porosity up to 50%.

Apparent bulk density (ρ) was determined by Archimedes displacement in ethanol.

Ultrasonic experiments were carried out at room temperature using a *Sofranel* equipment. The emitter (*Microscan* transducer from *Panametrics,* 6 mm in diameter) generates short pulses at 10 MHz. We can work in echo mode (the same transducer is alternatively emitter and receiver) or in transmission mode (the emitter is on one side of the cylindrical sample and the receiver is on the other, parallel side) (Fig. 1). Acoustic coupling was insured by a gel whose high-viscosity avoids intrusion into the sample porosity.

The longitudinal wave velocity is deduced from the flying time (τ) which corresponds to one travel through the specimen. In echo mode:

$$v_l = \frac{2L}{\tau} \qquad \text{Eq. (3)}$$

For ultrasonic experiments, “infinite medium” requires specimen dimensions (L) much larger than wavelength (λ) (Eq. (4)) and average size of heterogeneities (D_h) much lower than wavelength (Eq. (5)):

$$L >> \lambda \qquad \text{Eq. (4)}$$

$$D_h << \lambda \qquad \text{Eq. (5)}$$

For a frequency of 10 MHz, Eq. (4) is valid in all the cases we have considered, since λ is 0.2-0.4 mm whereas L is 17 mm ± 2 mm. Eq. (5) is verified in paste specimens, but is not verified in mortar and microconcrete samples where sand particles can be as large as 0.6 mm. This means the data related to mortars and microconcretes are more questionable than those related to pastes.

2.6. Mercury Intrusion Porosimetry (MIP)

The determination of pore volume versus pore radius was done using a *Carlo Erba* porosimeter (*series 2000 WS*). The porous sample was first put inside the glass dilatometer of a *Macropore Unit Model 120* (*Carlo Erba*). The dilatometer was vacuumed, to allow sample degassing, then filled with mercury. External pressure was incrementally increased up to 2,000 bars to force mercury to penetrate porosity.

Washburn’s equation (Eq. (7)) relates the pressure (p, in bars) to pore radius (r, in Å), surface tension of mercury (σ = 480 mN.m^{-2}), and wetting angle (θ = 141.3°):

$$p \cdot r = 2\sigma \cdot \cos\theta \qquad \text{Eq. (7)}$$

For cylindrical pores, Eq. (7) becomes (8):

$$r = \frac{7.5.10^4}{p} \qquad \text{Eq. (8)}$$

By plotting integrated pore volume vs. pore radius, it is possible to draw the cumulative distribution of pore volume.

The pressure range we used allows the mercury to enter pores from 3.7 nm to 7,500 nm. Only open porosity can be accessed. At high pressures, however, the walls of closed pores can be broken and closed pores become open pores.

2.7. Other characterizations

Powder XRD patterns were recorded using a *Philips PW-1729* diffractometer in Bragg-Brentano configuration. The angular deviation was ranging from 10 to 90° (in 2θ), by steps of $0.02°.s^{-1}$.

Thermal analyses (DTA and TG) were carried out using a *Thermal Analyst Instruments SDT 2960* apparatus. Heating rate was $5°C.min^{-1}$ from room temperature to 1000°C, in air, with alumina as internal standard.

Scanning electron microscopy was conducted using a *JEOL JSM-5200* microscope equipped with an *Oxford Instruments* EDX analyser.

3. Results and discussion

3.1. Effects of temperature

The main events that are expected to occur in heated concretes are as follows [7]:

- From room temperature to 120°C-200°C, there is vaporization of free and adsorbed water.
- Between 450°C and 500°C, portlandite loses water to give free lime:

$$Ca(OH)_2 \rightarrow CaO + H_2O$$

- In concrete with siliceous aggregate, the transformation of α-quartz to β-quartz occurs at T = 573°C. This transformation is accompanied by a volume expansion of ~ 1%, which can initiate cracking.

- In the range 600°C-700°C, the reactions that follow the decomposition of various calcium silicate hydrates (for example jennite or tobermorite-like phases) can generate new phases, such as β-C_2S, as mentioned by Lin et al [8].

- Between 700°C and 900°C, calcite (the main component of calcareous aggregate) decomposes to free lime:

$$CaCO_3 \rightarrow CaO + CO_2$$

As far as mechanical properties are concerned, both stiffness (Young's modulus, E) and fracture strength (σ_F) are affected [1,2]. Three domains can be distinguished [9]:

- From room temperature to ~ 400°C, high-strength concrete (HSC) show lower strength loss (l to 10%) than normal-strength concrete (NSC) (15%).

- From ~ 400°C to ~ 800°C, strength loss is severe in both HSC and NSC, although HSC keep a better resistance than NSC.

- For temperatures above ~ 800°C, residual strength has marginal value in both materials.

3.2. Thermal analyses

Thermal analysis data confirm the sequence of events described in § 3.1.

In pastes (2NP-28d, see Fig. 2), the DTA+TG curves show two main events, labeled as "1" (departure of free and adsorbed water, ~ 125°C) and "2" (dehydration of portlandite, ~ 450°C). Both events are associated with a weight loss. Between 650°C and 700°C, there is a third event (labeled as "3"), of small amplitude, also associated with a weight loss. One possibility would be elimination of hydroxyl residues. Complementary experiments are currently carried out to elucidate this point, using DTA+TG coupled with mass spectroscopy.

In siliceous microconcrete (3OS-7d, see Fig. 3), there are four events, with the third one ("3") related to the α-to-β quartz transformation at 573°C.

In calcareous mortars (5NC-28d, see Fig. 4) the decarbonation of calcite ("3") is responsible for an endothermic peak between 700°C and 800°C, associated with a large weight loss.

3.3. Young's modulus

Ultrasonic measurements show excellent reproducibility. For samples coming from a given batch (cement paste, mortar, or microconcrete), the scattering is always below 3%, in echo mode and in transmission mode as well.

Cement pastes

In pastes cured for 7 days, the acoustic velocities (Fig. 5) are ranked according to $v_l(2NP) > v_l(3NP) > v_l(5NP)$, whatever the temperature of treatment. This confirms that stiffness increases as w/c decreases, that is as porosity decreases.

An increase in the temperature of thermal treatments results in a decrease in Young's modulus. Four main domains can be distinguished:

1. Near 80°C, which is the lowest temperature investigated, free water evaporates and porosity increases, which leads to a drop in E.
2. From 80°C to a temperature T*, E does not change very much. The value of T* increases as w/c decreases. T* is ~ 250°C for w/c = 0.50, ~ 300°C for w/c = 0.35, and ~ 400°C for w/c = 0.25.
3. From T* to 600°C, E continues to decrease. This fact is thought to be connected with the decomposition of portlandite.
4. At temperatures above ~ 800°C, however, E regains higher values, because of presumed sintering phenomena.

When compared with pastes cured for 7 days, pastes cured for 28 days have lower porosity and higher CSH content. This causes higher cohesion, higher strength [10], and higher Young's modulus (Fig. 6). As far as the effects of thermal treatments are concerned, the main difference occurs in domain n°3, where the drop in E as temperature increases is larger in 28 d-cured pastes than in 7 d-cured pastes. Moreover, the value of E after treatment at 1000°C is lower in the former materials than in the latter.

Pastes with w/c of 0.25 (2NP series) have acoustic velocities that are 20-30% higher than those of pastes with w/c of 0.50 (5NP series). This difference of 20-30% is lower than it was found in 7 d-cured pastes, which shows the influence of the w/c ratio is particularly marked in the initial stages of cement setting and hardening.

Mortars and microconcretes

In mortars and microconcretes cured for 7 days, Young's modulus continuously decreases as the temperature of thermal treatment increases up to 800°C.

For temperatures below 300°C, the acoustic velocity is greater in mortars than in the corresponding pastes with same w/b and same thermal treatment. For temperatures above 300°C, however, the drop in E is larger in mortars than in cement pastes. This is also true when comparing 3OS-microconcretes with 3NP-pastes, but is not true when comparing 2OS-microconcretes which 2NP-pastes. Finally, when the temperature of treatment is very high (T > 800°C), the sintering phenomena cause a large increase in acoustic velocity and Young's modulus, as observed in pastes.

The results for mortars and microconcretes cured for 28 days (Fig. 7) are qualitatively similar to those for materials cured for 7 days. As for pastes, the 28 d materials exhibit higher values of E than the 7 d corresponding materials.

Ultrasonic evaluation becomes more and more difficult as the specimens are more and more cracked. For the calcareous mortars, which are the most sensitive to thermal damage, measurement becomes impossible when the temperature of treatment exceeds 600°C. For the microconcretes with silica fume (2OS and 3OS), which are the most resistant to thermal damage, measurement is still possible after treatment at 1000°C.

A very interesting point is that all materials (pastes, mortars, and microconcretes, whatever their w/b ratio) behave in a similar manner when one considers the ratio of E(T) to E_0, where

E(T) is Young's modulus after treatment at temperature T and E_0 the initial modulus (Fig. 8 and 9). Even if the calcareous mortars did not obey the law as well as the other materials, this fact suggests the existence of a common "guiding curve".

3.4. Porosity

Thermal treatments result in an increase in both total porosity (Fig. 10) and pore size (Fig. 11). For the highest temperatures that have been investigated, however, there is a slight decrease in total porosity. This effect can be attributed to sintering phenomena [11].

3.5. Microstructure

Thermal treatments cause cracking (examples are given in photos 1 to 5), but sintering phenomena may allow crack healing in materials submitted to very high temperatures (1000°C). The w/c or w/b ratios have a marked influence. For cement pastes with w/c = 0.50, the 7 d-cured samples are densely cracked after treatment at 700°C whereas the 28 d-cured samples are densely cracked after treatment at 500°C only. As previously mentioned, ultrasonic measurement is impossible in such cracked materials. For mortars, cracking becomes visible at temperatures around 300°C, then develops during stage 3, as defined in § 3.3. The calcareous mortars are more sensitive to cracking than the siliceous ones. The former are densely cracked after treatment at 500°C (7 d-cured materials) and 600°C (28 d-cured materials), whereas the latter show modest cracking after treatment at 600°C.

4. Conclusion

1. The ultrasonic method has been used for studying damage in cement-based materials (pastes, mortars, and microconcretes) which had been subjected to cumulative thermal treatments, at temperatures up to 1000°C. The method is simple, rapid, sensitive, and reproducible.

2. Room-temperature Young's modulus decreases when the temperature of treatment increases. Four main domains have to be taken into account, namely i) from room temperature to ~ 80°C, ii) from ~ 80°C to T*, where T* increases from ~ 250°C to 400°C, when w/c decreases, iii) from T* to ~ 600°C, and iv) T > ~ 600°C.
3. High-temperatures (T > 800°C) allow Young's modulus to regain, however, which is thought to be due to sintering phenomena.
4. All materials (pastes, mortars, and microconcretes, whatever their w/b ratio) exhibit similar relative changes in Young's modulus (E/E_0) versus temperature of thermal treatment. This may suggest the existence of a "guiding curve" that would be controlled by the common component, that is the cement itself. This point is currently being under investigation.
5. Porosity and pore size increase as temperature increases up to 700°C. At higher temperatures, sintering phenomena yields densification.
6. It must be pointed out again that the aim of the study was to collect materials data, in order to characterize small specimens, not too far from thermal, chemical, physical, and microstructural equilibrium. The results cannot be directly extrapolated to bulk parts, where we also have to take into account gradients in temperature, heterogeneity of microstructure and chemical composition, migration of water vapor [5], and mechanical constraints due to metallic reinforcement. However, the study of concrete parts subjected to high-temperature conditions cases always requires materials data, in particular Young's modulus data, to help us understand experimental results related to bulky specimens or to feed analytical or numerical models.

Acknowledgements

The study has been supported by *Association Technique de l'Industrie des Liants Hydrauliques* (*ATILH*).

References

[1] F.-J. Ulm, O. Coussy, Z. P. Bazant, The “Chunnel” Fire. I: Chemoplastic softening in rapidly heated concrete. J Eng Mech (March 1999) 272-282.

[2] F.-J. Ulm, P. Acker, M. Levy, The “Chunnel" Fire. II: Analysis of concrete Damage. J Eng Mech (March 1999) 283-289.

[3] G. Sanjayan, L.J. Stocks, Spalling of high-strength silica fume concrete in fire. ACI Mat J 90 (2) (1993) 170-173.

[4] D. P. H. Hasselman, Thermal Stress Resistance of Engineering Ceramics. Mat Sc Eng 71 (1985) 251-264.

[5] P. Kalifa, F.-D. Menneteau, D. Quenard, Spalling and pore pressure in HPC at high temperatures. Cem Concr Res 30 (2000) 1915-1927.

[6] N. Richard, Structure et propriétés élastiques des phases cimentières à base de mono-aluminate de calcium. Ph.D. Thesis in "Science des Matériaux "of University Paris VI, Paris, Feb. 1996.

[7] A. Feraille-Fresnet, Le rôle de l’eau dans le comportement à haute température des bétons. Ph.D. Thesis of Ecole Nationale des Ponts et Chaussées, Paris, Jan. 2000.

[8] W.-M. Lin, T. D. Lin, L. J. Powers-Couche, Microstructures of Fire-Damaged Concrete. ACI Mat J (May-Jun. 1996) 199-205.

[9] Y. N. Chan, G. F. Peng, M. Anson, Residual strength and pore structure of high strength concrete and normal strength concrete after exposure to high temperatures. Cem Concr Comp 21 (1999) 23-27.

[10] E. E. Hekal, Effect of Silica Fume on Physicochemical and Mechanical Properties of Hardened Cement Pastes : I- Hydration Kinetics, Phase Composition and Compressive Strength. Sil Ind, 64 (9-10) (2000) 163-167.

[11] J. Piasta, Z. Sawicz, L. Rudzinski, Changes in the structure of hardened cement paste due to high temperature. Mater Constr (Paris) 17 (100) (1984) 291-295.

Photo 1: Cracking after treatment at 400°C

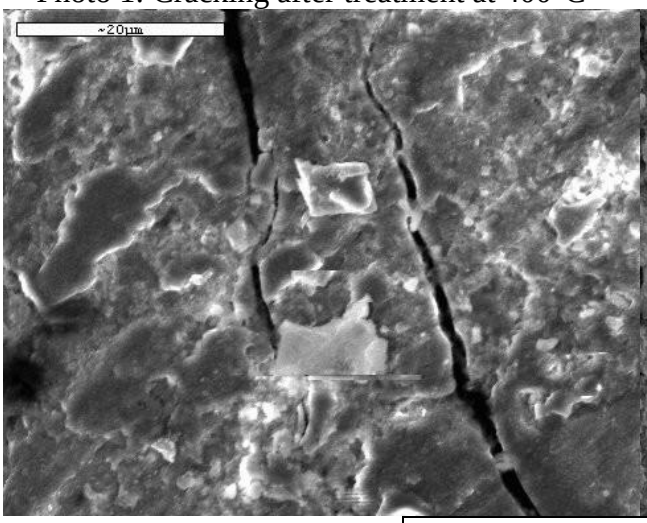

Photo 2: Cracking after treatment at 700°C

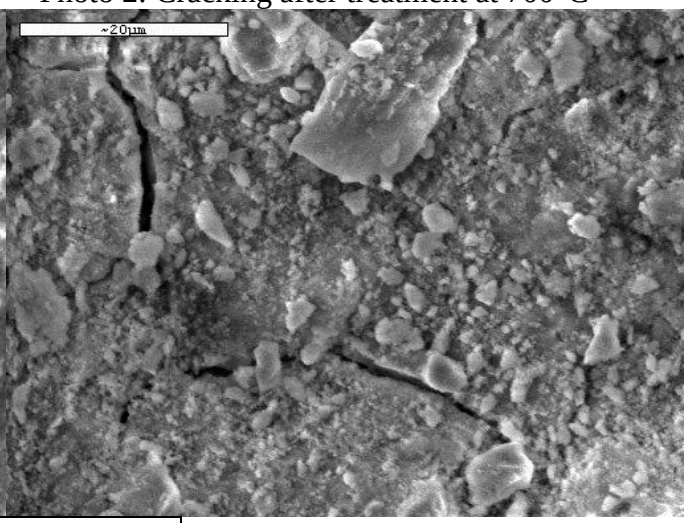

Paste, E/C = 0.25, cure = 7 days

Photo 3: 600°C

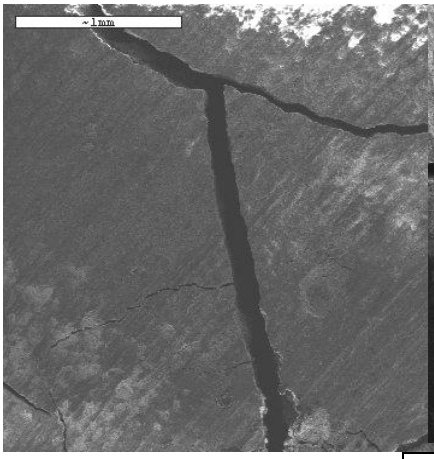

Photo 4: 800°C

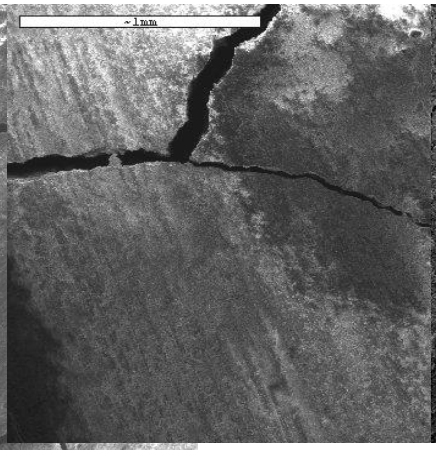

Photo 5: 1000°C

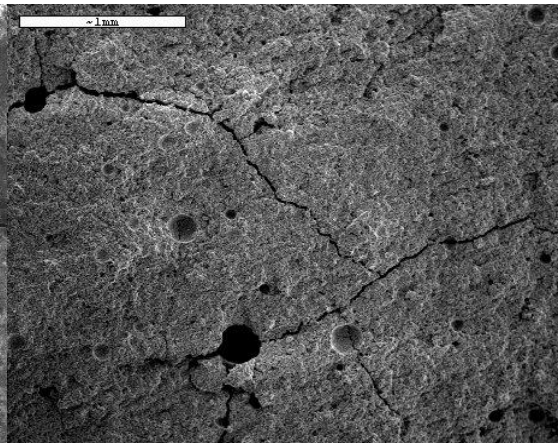

Paste, E/C = 0.50, cure = 7 days

Table 1: Chemical composition of the cement (CPA CEM I)
(% by weight)

SiO_2	Al_2O_3	Fe_2O_3	CaO	SO_3	K_2O	MgO	Na_2O	Free lime	Ignition loss
20	5.3	2.5	64	3.2	1	1	0.15	0.7	2.4

Table 2: Bogue's composition of the cement
(% by weight)

C_3S	C_2S	C_3A	C_4AF
61.5	10.5	10	7.5

Table 3: Nomenclature

Material	paste	paste	paste	mortar	mortar	mortar	concrete	concrete
Sand nature	---	---	---	siliceous	siliceous	calcareous	siliceous	siliceous
Silica fume	---	---	---	---	---	---	SF	SF
Water/binder	0.25	0.35	0.50	0.35	0.50	0.50	0.25	0.35
Sample code	2NP	3NP	5NP	3NS	5NS	5NC	2OS	3OS

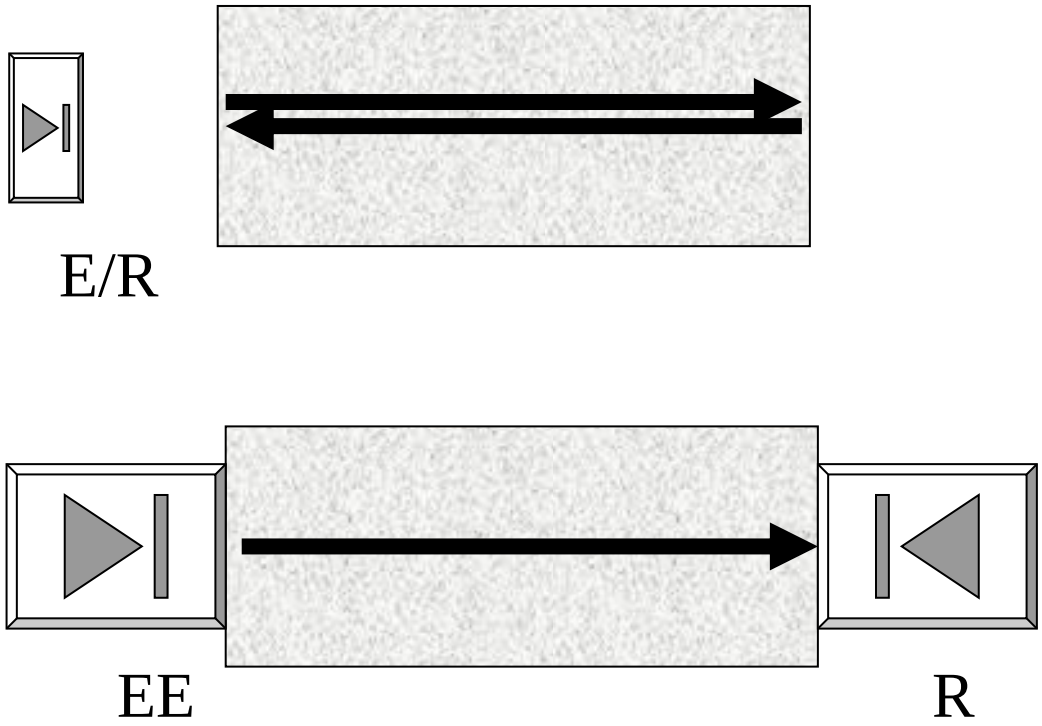

Fig. 1: Ultrasonic methods. E is the emitter and R the receiver.
Echo mode (top) and transmission mode (bottom).

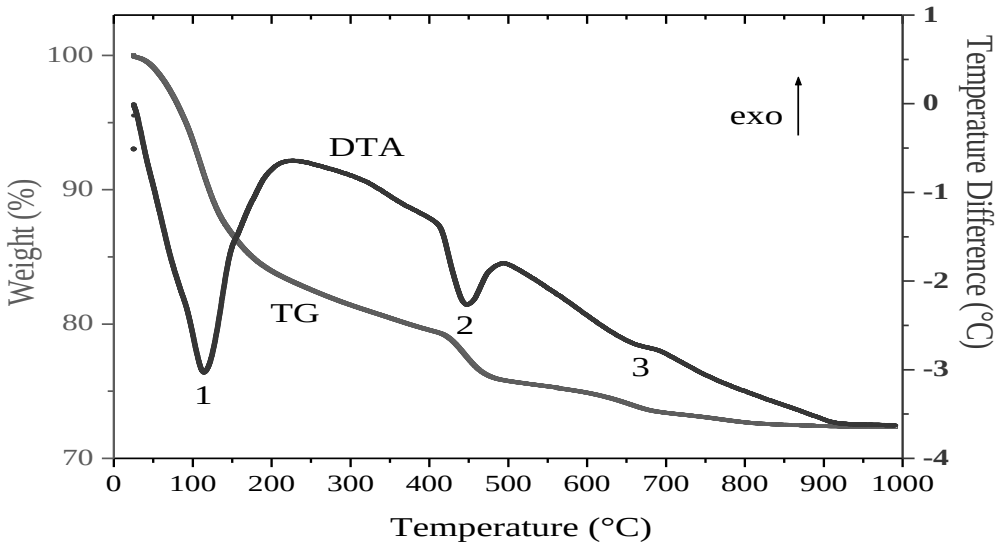

Fig. 2: DTA/TG of material 2NP28 000.
(Paste, E/C = 0.25, cure = 28 days).

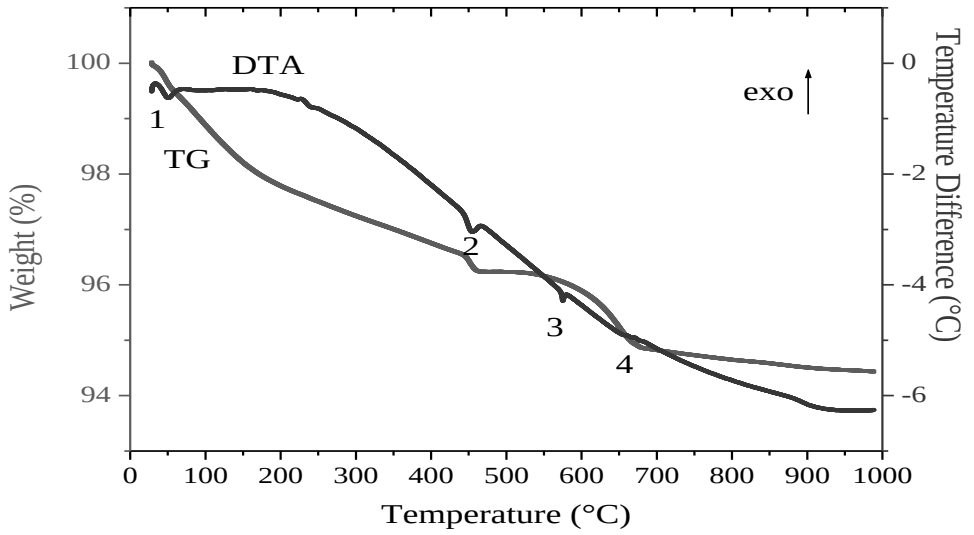

Fig. 3: DTA/TG of material 3OS7 080.
(Microconcrete with siliceous sand and fume silica, E/C = 0.35, cure = 7 days).

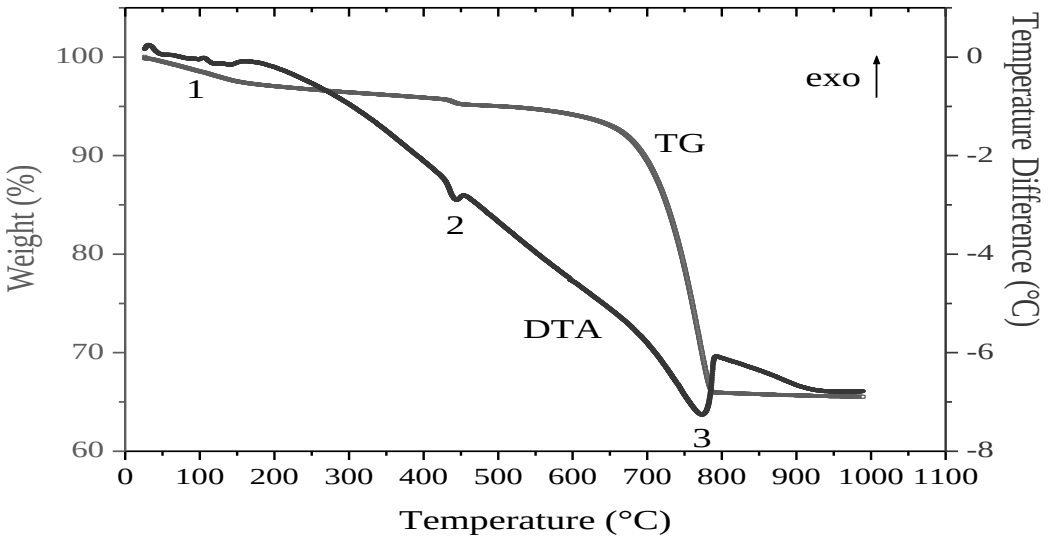

Fig. 4: DTA/TG of material 5NC28 080.
(Mortar with calcareous sand, E/C = 0.50, cure = 28 days).

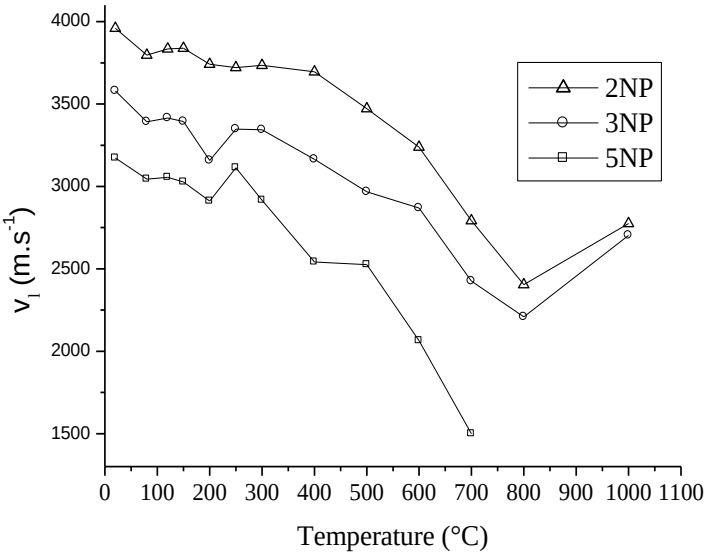

Fig. 5: Pastes, cure = 7 days.
Acoustic longitudinal velocities (v_l) versus soaking temperature.

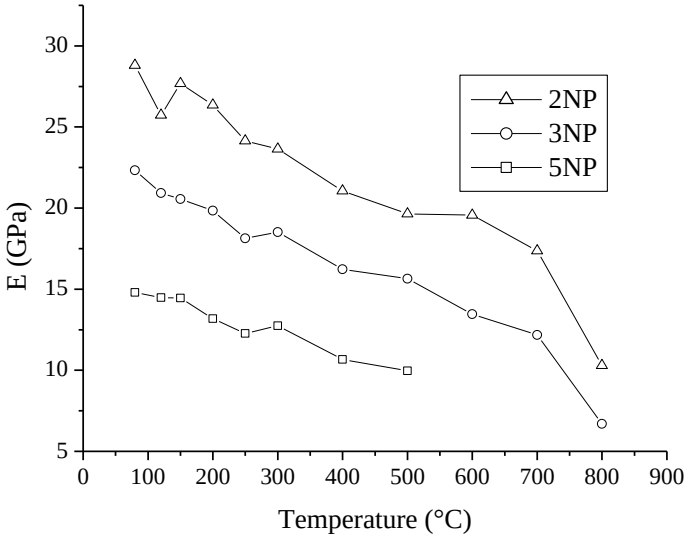

Fig. 6: Pastes, cure = 28 days.
Room-temperature Young's modulus (E) versus soaking temperature.

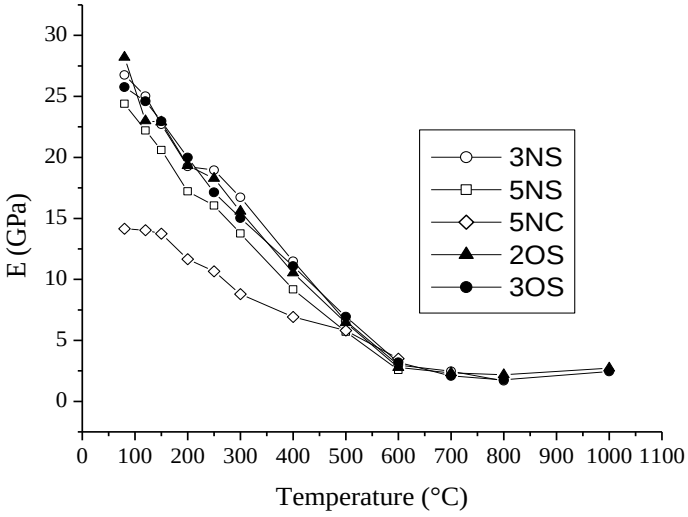

Fig. 7: Mortars and microconcretes, cure = 28 days.
Room-temperature Young's modulus (E) versus soaking temperature.

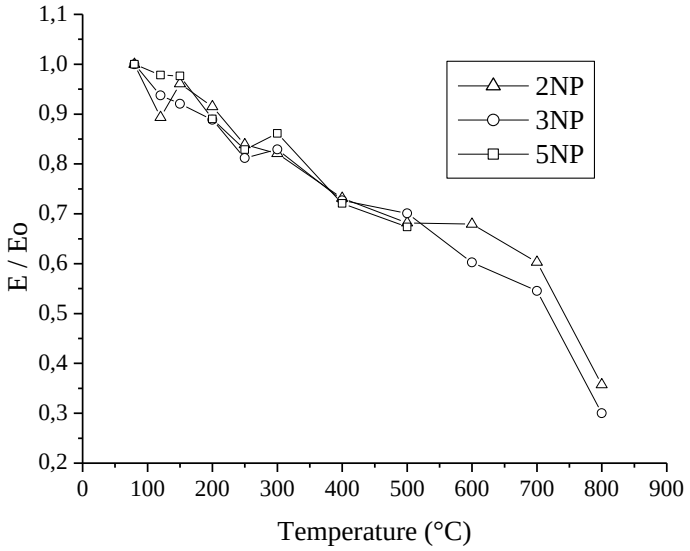

Fig. 8: Pastes, cure = 28 days.
E/E_0 versus soaking temperature (E_0 is initial Young's modulus).

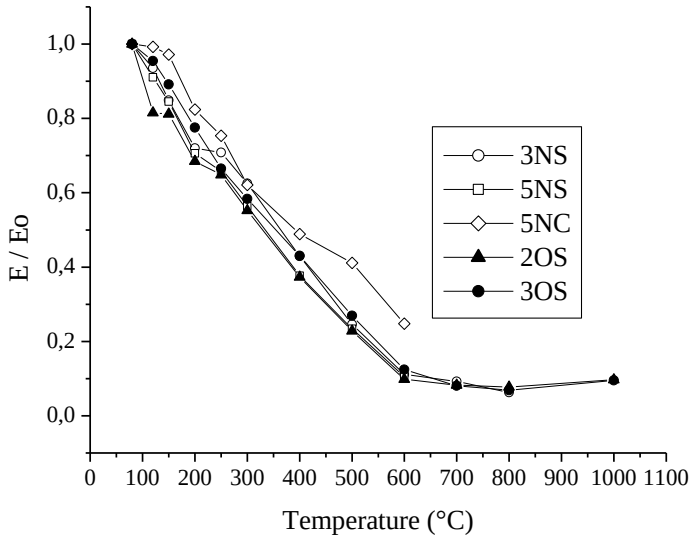

Fig. 9: Mortars and microconcretes, cure = 28 days.
E/E_0 versus soaking temperature (E_0 is initial Young's modulus).

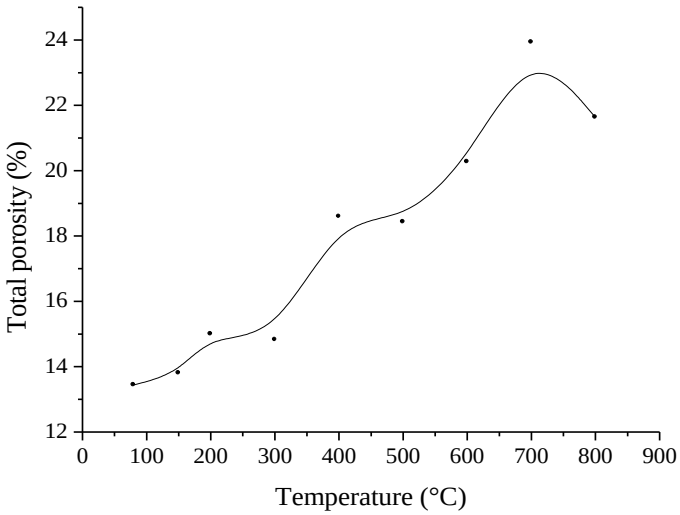

Fig. 10: Siliceous microconcrete: Total porosity versus soaking temperature.

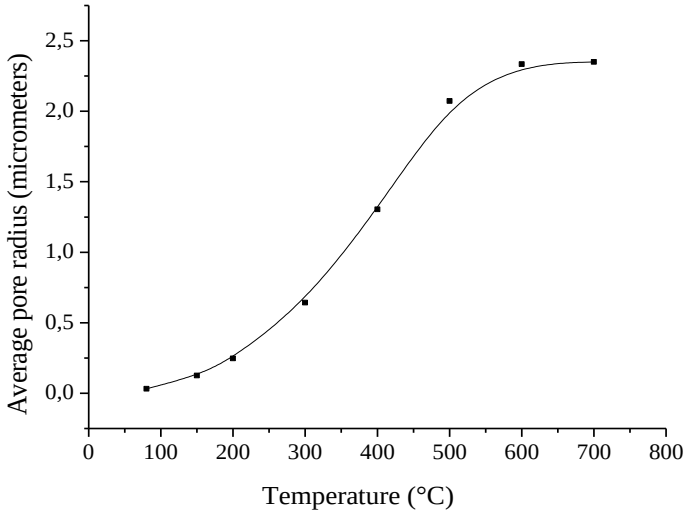

Fig. 11: Siliceous microconcrete: Average pore size versus soaking temperature.